View metadata, citation and similar papers at core.ac.uk
brought to you by CORE
provided by Directory of Open Access Journals

Processing and Application of Ceramics 5 [3] (2011) 139–147

Effect of oxidizing and reducing atmospheres on $Ba(Ti_{0.90}Zr_{0.10})O_3$:2V ceramics as characterized by piezoresponse force microscopy

Francisco Moura[1], Alexandre Z. Simões[2,*], Carla S. Riccardi[3], Maria A. Zaghete[3], Jose A. Varela[3], Elson Longo[3]

[1]*Universidade Federal de Itajubá- UNIFEI - Campus Itabira, Rua São Paulo 377, Bairro Amazonas, P.O. Box 355, 35900-37, Itabira, Minas Gerais, Brazil*

[2]*Universidade Estadual Paulista- UNESP – Faculdade de Engenharia de Campus Itabira, Av. Dr Ariberto Pereira da Cunha 333, Bairro Pedregulho, P.O. Box 355, 12516-410, Guaratinguetá, São Paulo, Brazil*

[3]*Laboratório Interdisciplinar em Cerâmica, Instituto de Química, Universidade Estadual Paulista, P.O. Box 355, 14801-907 Araraquara, São Paulo, Brazil*

Received 18 January 2011; received in revised form 23 May 2011; accepted 18 June 2011

Abstract

The effect of annealing atmospheres (At_{amb}, N_2 and O_2) on the electrical properties of $Ba(Ti_{0.90}Zr_{0.10})O_3$:2V (BZT10:2V) ceramics obtained by the mixed oxide method was investigated. X-ray photoelectron spectroscopy (XPS) analysis indicates that oxygen vacancies present near Zr and Ti ions reduce ferroelectric properties, especially in samples treated in an ambient atmosphere (At_{amb}). BZT10:2V ceramics sintered in a nitrogen atmosphere showed better dielectric behaviour at room temperature with a dielectric permittivity measured at a frequency of 10 kHz equal to 16800 with dielectric loss of 0.023. Piezoelectric force microscopy (PFM) images reveal improvement in the piezoelectric coefficient by sintering the sample under nitrogen atmosphere. Thus, BZT10:2V ceramics sintered under a nitrogen atmosphere can be useful for practical applications which include nonvolatile digital memories, spintronics and data-storage media.

Keywords: *ferroelectrics, powder metallurgy, X-ray diffraction, dielectric response*

I. Introduction

Diffuse phase transition (DPT) is an interesting topic in ferroelectric physics. A typical characteristic of DPT is the relaxor behaviour which occurs in a ferroelectric phase transition, predominantly in perovskite structure materials, especially in lead compounds, such as PMN, PSN and PLZT. DPT was found in solid solutions of $BaTiO_3$ and $BaZrO_3$ (BTZ) which is one of the most important compositions for dielectrics in multilayer ceramic capacitors [1], because the Zr ion has higher chemical stability than the Ti [2,3] ion and the high permittivity of the $BaTiO_3$ ceramics increases with addition of zirconium. The sintering temperature of BZT is up to 1300°C. By doping with Zr, the sintering temperature will increase, and the dielectric constant will rise [4]. When the ratio of Zr to Ti in BZT reaches 20%, the Curie temperature is at room temperature (around 300 K), which is the ideal material for preparing variable electric capacities [5]. Chen suggested [6] that these features of relaxor phenomena are not caused by elementary excitation or the typical dielectric sources, (space charge), but by the reminiscence of a broad first-order phase transition obscured by severe geometrical and compositional randomness. However, there are some theories which consider the origin of high relaxor dielectric permittivity as the space charges arising from defects or vacancies [7,8]. Therefore, a material doped with aliovalent components would have higher dielectric permittivity. It is known that the doping is an effective way to improve the material performance in electroceramics. A donor dopant, such as Va^{5+} induces cationic defects while occupying the B site of the perovskite lattice [9,10]. This behaviour may cause sever-

* Corresponding author: tel: +55 12 3123 2765
fax: +55 12 3123 2800, e-mail: *alezipo@yahoo.com*

al effects on the dielectric behaviour through interaction with domain walls [11,12]. Similar to Zr modified BT, BZT10:2V ceramics may be a promising material as a lead-free actuator. In previous work, we investigated the dielectric characteristics of BZT10:2V ceramics [13,14]. We observed that the substitution of vanadium on the B-site broadens the dielectric permittivity curves due to repulsion of vanadium with their next nearest neighbours leading to a structure which is tetragonally distorted. X-ray photoemission spectroscopy (XPS) is among the most suitable technique for investigating the effects of surface layers on the polarization properties and piezoelectric behaviour of polycrystalline ceramics [15]. The method of mixed oxide reactions is a good choice for the ceramic powder preparation which is important in the formation of highly dispersed phased materials typical for metal powders or oxide based materials or the formation of a new product by a solid-state reaction. In this method, there is an increase in the area of contact between the reactant powder particles due the high sintering temperature which allows contact of fresh surfaces. In addition, the high defect densities induced by the intensive temperature favour the diffusion process.

Thus, we report the preparation of BZT10:2V ceramics sintered under various atmospheres using the mixed oxide method. We have studied the effects of annealing atmospheres (oxygen, At_{amb} and nitrogen) on the nature of defects and electrical properties of BZT10:2V ceramics.

II. Experimental

$Ba(Zr_{0.10}Ti_{0.90})O_3$ ceramics were prepared by a solid-state reaction. High purity $BaCO_3$, TiO_2 and ZrO_2 starting materials were weighed and wet mixed in alcohol. After drying, the powders were calcined at 1200°C for 4 hours. Separately, vanadium oxide was dissolved in nitric acid and complexed with citric acid and ethylene glycol. The vanadium citrate solution was added to the $Ba(Zr_{0.10}Ti_{0.90})O_3$ powders and calcined at 600°C for 4 hours. BZT10:2V ceramics were sintered at 1200°C under nitrogen, oxygen and ambient atmospheres with pellets in a size of about 10 mm × 2 mm. The density of the sintered compacts was measured by the Archimedes method. X-ray diffraction data were collected with a Rigaku Rint 2000 diffractometer under the following experimental condition: 50 kV (voltage), 150 mA (current of X-ray tube), $20° \leq 2\theta \leq 80°$, $\Delta 2\theta = 0.02°$, λCuK_α monocromatized by a graphite crystal, divergence slit = 2mm, reception slit = 0.6mm, accumulation time per step = 10s. After sintering the disks were polished to 1 mm in thickness and characterized by electrical measurements. The densities of the ceramic samples sintered under nitrogen, oxygen and air atmospheres are 96, 92 and 87% of the theoretical density of BZT10:2V (6.260 g/cm^3). Gold electrodes were applied by evaporation through a sputtering system in a polished surface of the sintered discs.

The dielectric characterization was accomplished in an impedance analyser, Model 4192 of HP. Measurements of the capacitance as a function of temperature at several frequencies were conducted. From the capacitance dependence temperature curves, the Curie temperature was determined. Ferroelectric properties were measured on a Radiant Technology RT6600A tester system equipped with a micrometer probe station in a virtual ground mode. High-resolution photoelectron spectra were collected on a Physical Electronics PHI 1600/3057 spectrometer equipped with a monochromized Al-Kr (1486.6 eV) X-ray beam with detection normal to the surface. The spectrometer was operated in a fixed analyzer energy transmission mode, and the pressure during analysis was maintained at approximately 6.66×10^{-8} Pa. Photoelectron spectra of Zr *3d* and Ti *2p* core levels were recorded using a computer controlled data collection system. The electron analyzer was set at pass energy of 10 eV. Piezoelectric measurements were carried out using a setup based on an atomic force microscope in a Multimode Scanning Probe Microscope with Nanoscope IV controller (*Veeco FPP-100*). In our experiments, piezoresponse images of the samples were acquired in ambient air by applying a small ac voltage with amplitude of 2.5 V (peak to peak) and a frequency of 10 kHz while scanning the sample surface. To apply the external voltage we used a standard gold coated Si_3N_4 cantilever with a spring constant of 0.09 N/m. The probing tip with an apex radius of about 20 nm was in mechanical contact with the uncoated sample surface during the measurements. Cantilever vibration was detected using a conventional lock-in technique [16].

III. Results and discussion

Figure 1 illustrates the room temperature X-ray diffraction pattern obtained from BZT10:2V ceramics sintered at various atmospheres. The X-ray reflections show that the single phase with a tetragonal perovskite structure was obtained which is a clear indication that vanadium has formed a stable solid solution with the BZT lattice. Bragg reflections peaks are indicative of the perovskite structure which is mainly characterized by a higher intense peak (hkl-110) at $2\theta = 31°$ and no apparent peak splitting is identified. Regarding the role of an annealing atmosphere, it is evident that all samples showed good crystallinity with no second phase formation. Vanadium can replace either titanium or zirconium in the lattice. To confirm these results Rietveld analyses will be conducted.

The temperature dependence of dielectric permittivity and dielectric loss tan(δ) for three samples at 10 kHz is shown in Fig. 2a and 2b, respectively. The dielectric permittivity for ceramics sintered in nitrogen showed higher values compared to the ceramics sintered in At_{amb}

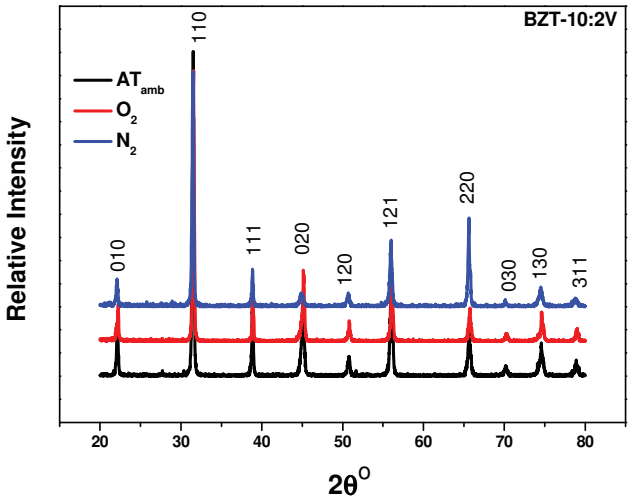

Figure 1. X-ray diffraction data for BZT10:2V ceramics sintered at 1200°C for 2 hours in a conventional furnace under N_2, O_2 and At_{amb} atmospheres

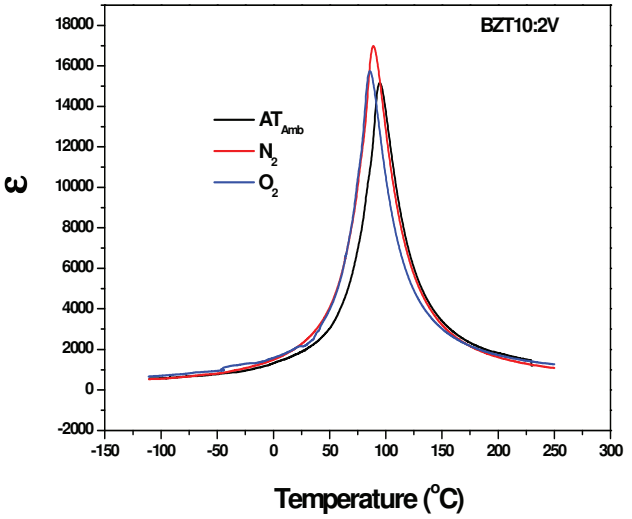

a)

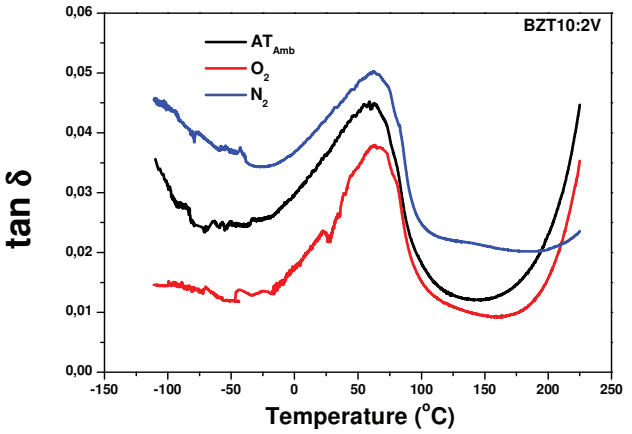

b)

Figure 2. Temperature dependence of: a) dielectric permittivity and b) dielectric loss at 10 KHz for BZT10:2V ceramics sintered at 1200°C for 2 hours under N_2, O_2 and At_{amb} atmospheres

and oxygen atmospheres. Regarding dielectric loss, the measurements suggest that low frequency loss values are significantly higher in a nitrogen atmosphere which can be explained by the higher space charge concentration which again arises due to a higher oxygen vacancy concentration. Also, it can be noted that dielectric properties (both the dielectric permittivity and the dielectric loss) of oxygen and At_{amb} do not improve appreciably whereas nitrogen sintered ceramics show a significant improvement in the dielectric properties which again emphasizes the superior quality of nitrogen sintered ceramics. It is possible that this decrease in the permittivity for oxygen and At_{amb} atmospheres is caused by space charge polarization which is inherently related to the non-uniform charge accumulation. The dielectric permittivity increases gradually with an increase in temperature up to the transition temperature (T_c) at Curie point, and then decreases due to the relatively large ionic radius of the B ion which enhances the thermal stability of BO_6 octahedra when compared to Ti or Zr [17–19]. Also, the BO_6 octahedra packing density will be determined by the size of the B ion. Larger B ions produce more closely packed octahedral which are therefore, more stable. The V^{5+} centre enters into the B-site of the ABO_3 perovskite lattice leading to a charged $[VO_6]^{\bullet}$ defect which is associated with a barium vacancy in a local barium cluster $[V''_{Ba}O_{12}]$. This result is in agreement with Rietveld analyses and will be published later. In fully or partly ionic compounds, vacancies are charge balanced by other defects which form an overall neutral system. It can be assumed that particle charge compensation occurs at a nearest-neighbour barium cluster site in the $[BaO_{12}]$ because the resulting coulomb interaction is the most important driving force. This assignment is in accordance with a first-principles calculation. Probably an equilibrium can be reached between "free" $[VO_6]^{\bullet}$ centres and $[VO_6]^{\bullet} + [V''_{Ba}O_{12}]$ associated defects. We can consider the free $[VO_6]^{\bullet}$ clusters as responsible for ionic mobility and $[VO_6]^{\bullet} + [V''_{Ba}O_{12}]$ defect dipole complexes as the main cause of electrical properties in the ceramic. Hence, charge transport will be considerably hindered. Below the Curie temperature, a high dependence of the dielectric loss was observed at elevated temperatures, vanadium doping stabilizes this dependence. The possible formation of dipole complexes may result in a reduced dielectric loss at elevated temperatures reflecting that good insulation resistance was maintained at high temperatures which is important for high temperature piezoelectric applications. The dielectric loss and dielectric permittivity show strong dependence as atmosphere changes. At the same frequency region, the obtained values are (0.023; 16880) (N_2); (0.034; 15650) (O_2) and (0.04; 14980) (At_{amb}). It is known that the increase in the dielectric loss is due to extrinsic resonance behaviour caused by defects (vacancy, movable ion, leaky grain boundary [20–29], etc.) that devel-

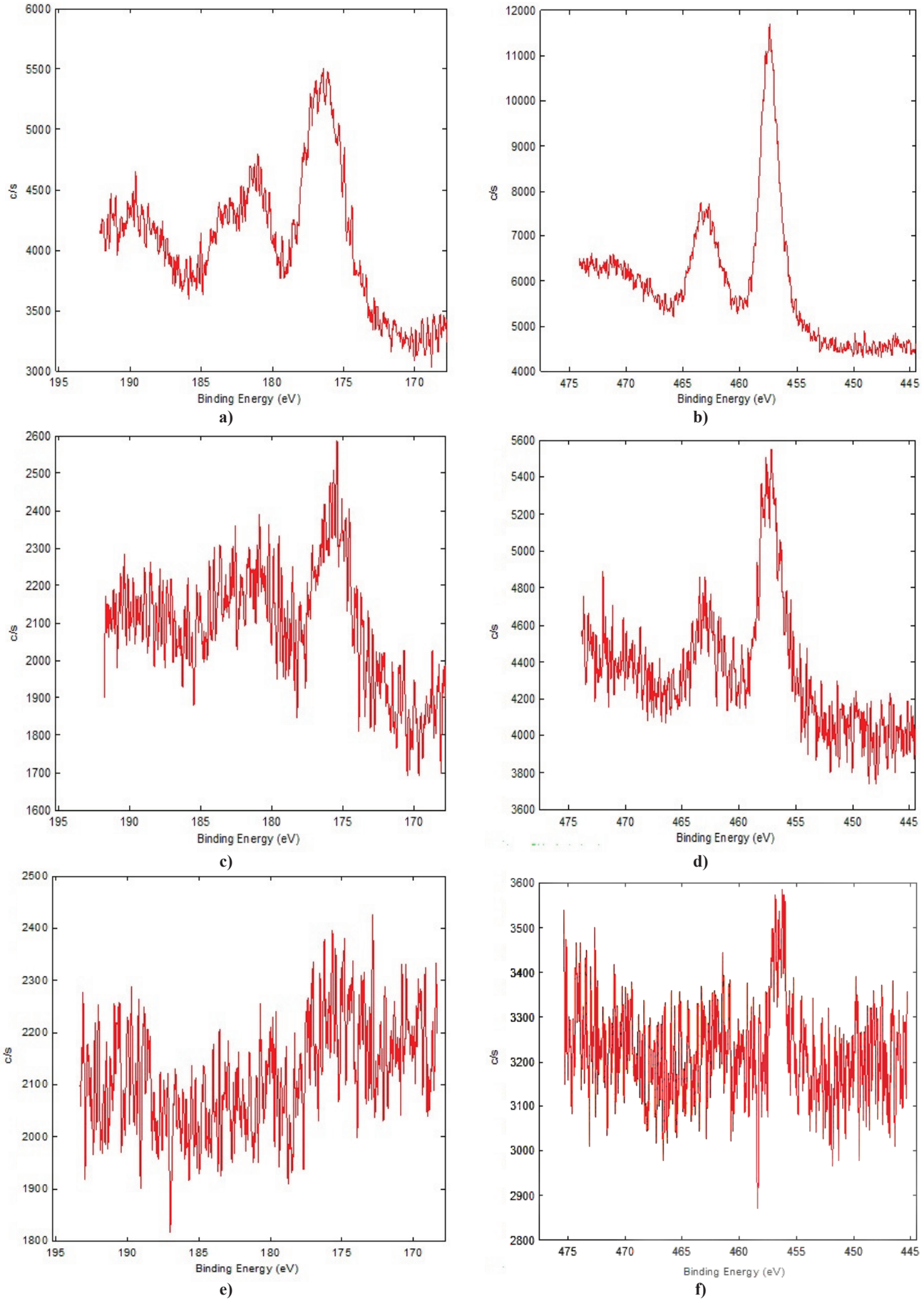

Figure. 3. XPS spectra of Zr*3d* and Ti*2p* peaks for BZT10:2V ceramics sintered at N_2 (a) and (b); O_2 (c) and (d) and At_{amb} (e) and (f) atmospheres

oped in the structure of the bulk material with changes in the sintering atmosphere. The sample sintered under a nitrogen atmosphere possesses a significant difference in the dielectric loss peak which suggests a pinch-off of the phase transition. Due to the fine-grain microstructure (not shown in the text) in the sample, the introduction of vanadium causes a more sensitive distortion of the perovskite lattice which leads to a reduction in the oxygen octahedron interstices. The distortion of the perovskite lattice can strengthen the structure fluctuation of BZT10:2V ceramics which can be account for different diffusion phase transition behavior characteristics in this sample.

$[ZrO_6]^x$, $[TiO_6]^x$, $[VO_6]^\bullet$ clusters are present in the BZT10:2V lattice. As the oxygen content is reduced, there is a charge transference of $[VO_6]^\bullet$ to the Ti and Zr clusters, according to the equations (1) and (2).

$$[VO_6]^\bullet + [ZrO_6]^x \rightarrow [VO_6]^x + [ZrO_6]^\bullet \quad (1)$$

$$[VO_6]^\bullet + [TiO_6]^x \rightarrow [VO_6]^x + [TiO_6]^\bullet \quad (2)$$

In these equations, clusters oriented in the centre symmetric structure are observed which change the internal polarization at the clusters level by improving the remnant polarization. As the oxygen content increases, the effects of polarization are reduced due to less random crystal growth. On the other hand, more crystalline ceramics produce better polarization aspects due to the association of $[ZrO_6]$ and $[TiO_6]$ charged clusters and the crystalline behaviour which possesses a more uniform charges distribution in the sample sintered under nitrogen atmosphere.

To gain a further understanding on the defects created by the sintering atmosphere in BZT10:2V ceramics, X-ray photoemission analysis was conducted. The photoemission of Zr *3d* and Ti *2p* core levels are shown in Fig. 3. Zr *3d* and Ti *2p* peaks for BZT10:2V ceramics sintered under nitrogen and oxygen atmospheres shifted toward the lower binding energy side with respect to the energy for the At_{amb} (Figs. 3a,b). The binding energies of Zr *3d* and Ti *2p* ceramics sintered under an At_{amb} remain identical with the standard values. However, the binding energy peaks of Ti and Zr changes with the sintering atmosphere. These experimental results clearly indicate that oxygen vacancies are preferably present near Zr and Ti ions. Furthermore, the peaks for states which are less oxidized than Ti^{4+} and Zr^{4+} are also located in a lower binding energy region. The peak broadening suggests that some oxygen atoms at the perovskite layers are removed which implies that oxygen vacancies could be induced in the neighbourhood of the Zr and Ti ions. Because the ferroelectric behaviour of those materials mainly originates from metal-oxygen octahedra, the reduction of the ferroelectric properties in the sample sintered under an air atmosphere is related to oxygen vacancies present at the titanium and zirconium oxygen octahedra. Therefore, there are three chemical states for

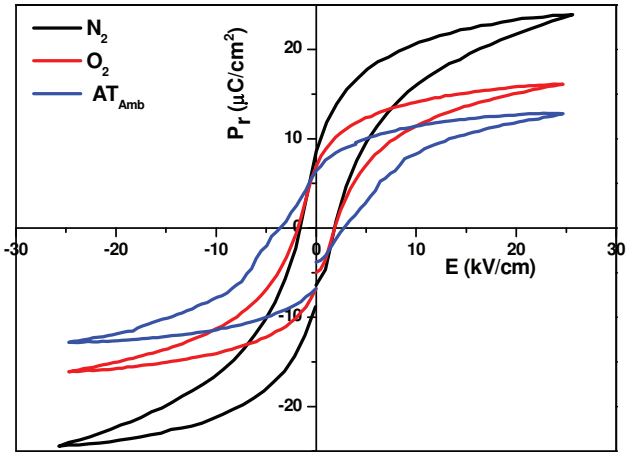

Figure. 4. Hysteresis loops for *BZT10:2V* ceramics sintered at 1200°C for 2 hours in a conventional furnace under N_2, O_2 and At_{amb} atmospheres

an oxygen anion in the vanadium doped barium zirconium titanate ceramics sintered at 1200°C. The chemical states of the oxygen anion will change with the annealing atmosphere, i.e. the solid solution compositions in the sample change which is similar to the ion radius of Ti, Zr, and V due to some substitutions of V^{5+} for Ti^{4+} or Zr^{4+} which result in a decrease in the oxygen binding energy.

Figure 4 shows the hysteresis loops (*P* vs *E*) measured at room temperature. Hysteresis loops reveal different saturation (P_s) and remnant polarization (P_r) values along sintering atmospheres. A sample sintered in a nitrogen atmosphere shows better polarization data than a sample sintered at ambient and oxygen atmospheres which implies that oriented micropolar clusters exist as a typical ferroelectric-relaxor characteristic. The lower remnant polarization of the samples annealed in oxygen and ambient atmospheres are caused by a trapped charge ($O_2^{''}$) associated with other defects ($V_0^{\bullet\bullet}$ or even defect dipole complexes such as oxygen vacancies associated with barium vacancies ($V^{''''}_{Ba}$ - $V_0^{\bullet\bullet}$) located in the grain boundary and in the film-electrode interface. The increased P_r of our sample annealed under a nitrogen atmosphere can be attributed to the structural change in the oxygen octahedron since the annealing atmosphere controls cation defects in the lattice. The *P-E* loop was actually not closed as a result of the high leakage current at higher electric fields of 25.0 kV/cm. Thus, the charge compensation required by addition of V^{5+} ions could be achieved by reducing oxygen vacancies which induces changes in the leakage current. It is also possible that BZT10:2V ceramics are free of imprint phenomena which cause a shift in the coercive field axis and leads to a failure in the capacitor. This failure can be caused by such defects as oxygen vacancies and space charges that leads to domain pinning and is almost absent in the BZT10:2V sample. Therefore, the role of vanadium is to reduce the stress within the domains [30] which re-

sults in low coercive field (E_c) of 2 kV/cm. Finally, the polarization behaviour shows that BZT10:2V ceramics annealed under a nitrogen ambient atmosphere could be promising for low-temperature ferroelectric and piezoelectric applications.

Piezoelectric behaviour at room temperature is shown in Fig. 5. The butterfly-shaped strain versus electric fields can be observed for different sintering atmospheres. The difference in the strain behaviour might be attributed to different domain configurations. As is usually observed in the relaxor-based "soft" piezoelectric materials, the hysteresis at low fields is attributed to domain motions. In the present work, the hysteresis could also be associated with the domain reorientation which is prominent for a sample with a multidomain state. Above 30 kV/cm, the hysteresis-free strain is observed which implies a poling state free of domain wall motions induced by the high external electric fields. At 60 kV/cm, (the highest electric field in the study), the piezoeletric coefficient is at a maximum level. The oxidant and reducing atmosphere increase the piezoeletric behaviour which in part is due to domain reorientation. Beyond that point, it is possible that a modest bias field results in the transition from an asymmetric phase to a symmetric phase. This field-induced phase transition may be ascribed to the pinching effect, that is, the consequent decrease in free energy difference among polymorphic phases. A careful inspection of the d_{33} -E plots reveals that there are two apparent linear regions at low fields (E < 30 kV/cm) and high fields (E > 70 kV/cm) and one transition region corresponding to domains reorientation induced by external electric fields. It is shown that BZT10:2V ceramic samples sintered in a nitrogen atmosphere showed higher piezoeletric strain than the sample sintered under an air atmosphere. The piezoelectric coefficient was 43 pm/V, 40 pm/V and 27 pm/V for BZT10:2V ceramics sintered under nitrogen, oxygen and air atmospheres, respectively. These results are generally observed phenome-

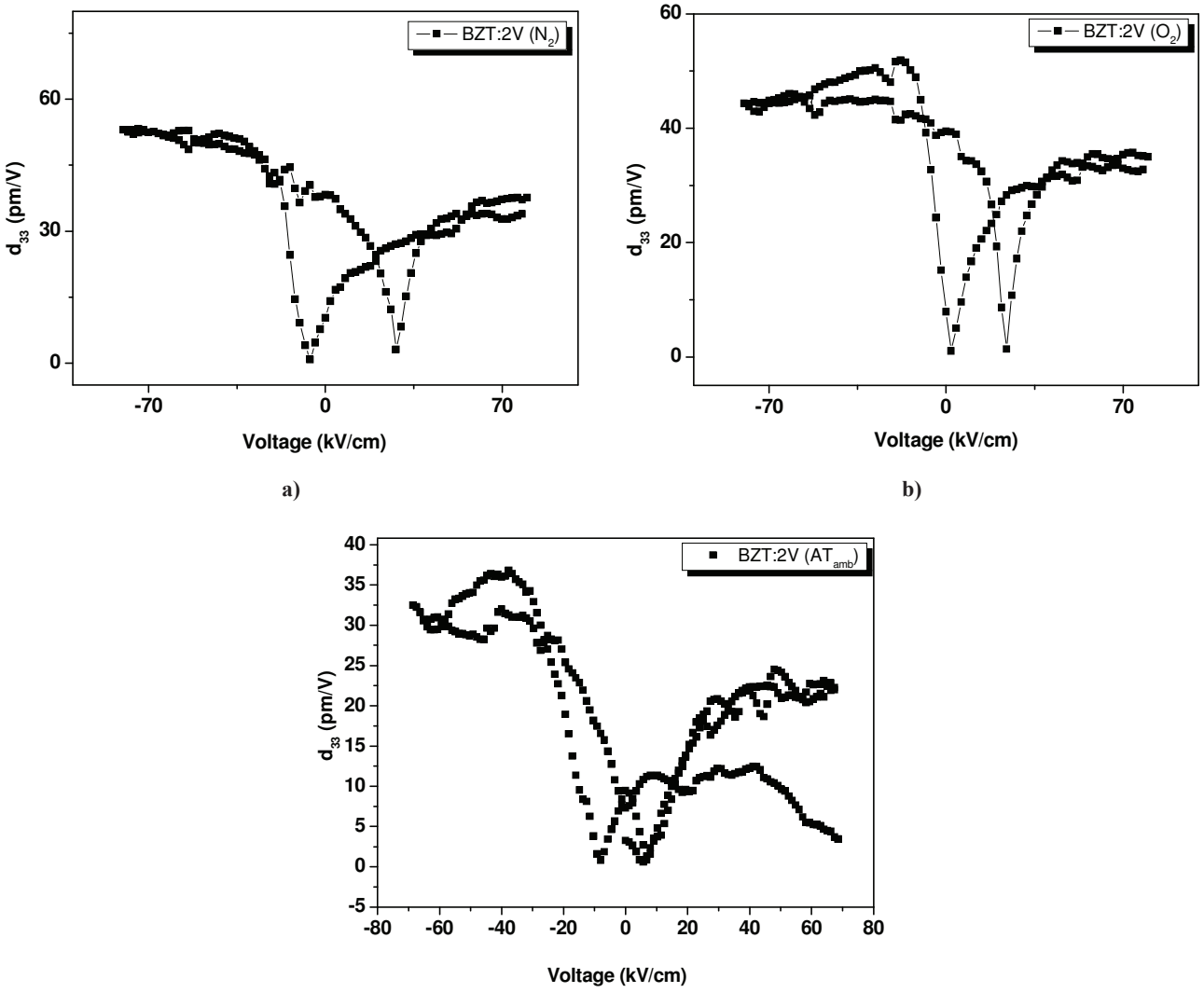

Figure 5. Piezoelectric coefficient as function of voltage for BZT10:2V ceramics sintered at 1200° C for 2 hours in a conventional furnace under: a) N_2, b) O_2 and c) At_{amb} atmospheres

non in electronic ceramics which might be attributed to the improved ceramic quality due to a small amount of impurity doping [31]. It is shown that vanadium improves the piezoelectric strain. The improvement in the piezoelectric response after doping can be associated with the better polarizability and the pinning effect. Thus, we can assume that the piezoelectric response was found to be closely related to the purity of the phase and grain size which suggests that the annealing atmosphere is of fundamental importance in the switching mechanism of the ceramics because in part the reduced grain sizes leads to an increase in the grain boundaries densities which makes contribution to the decreased domain walls mobility.

To visualize the role exerted by the atmosphere on the piezoresponse of BZT10:2V ceramics we constructed domain ceramic structures. The results were observed by piezoelectric force microscopy (PFM)

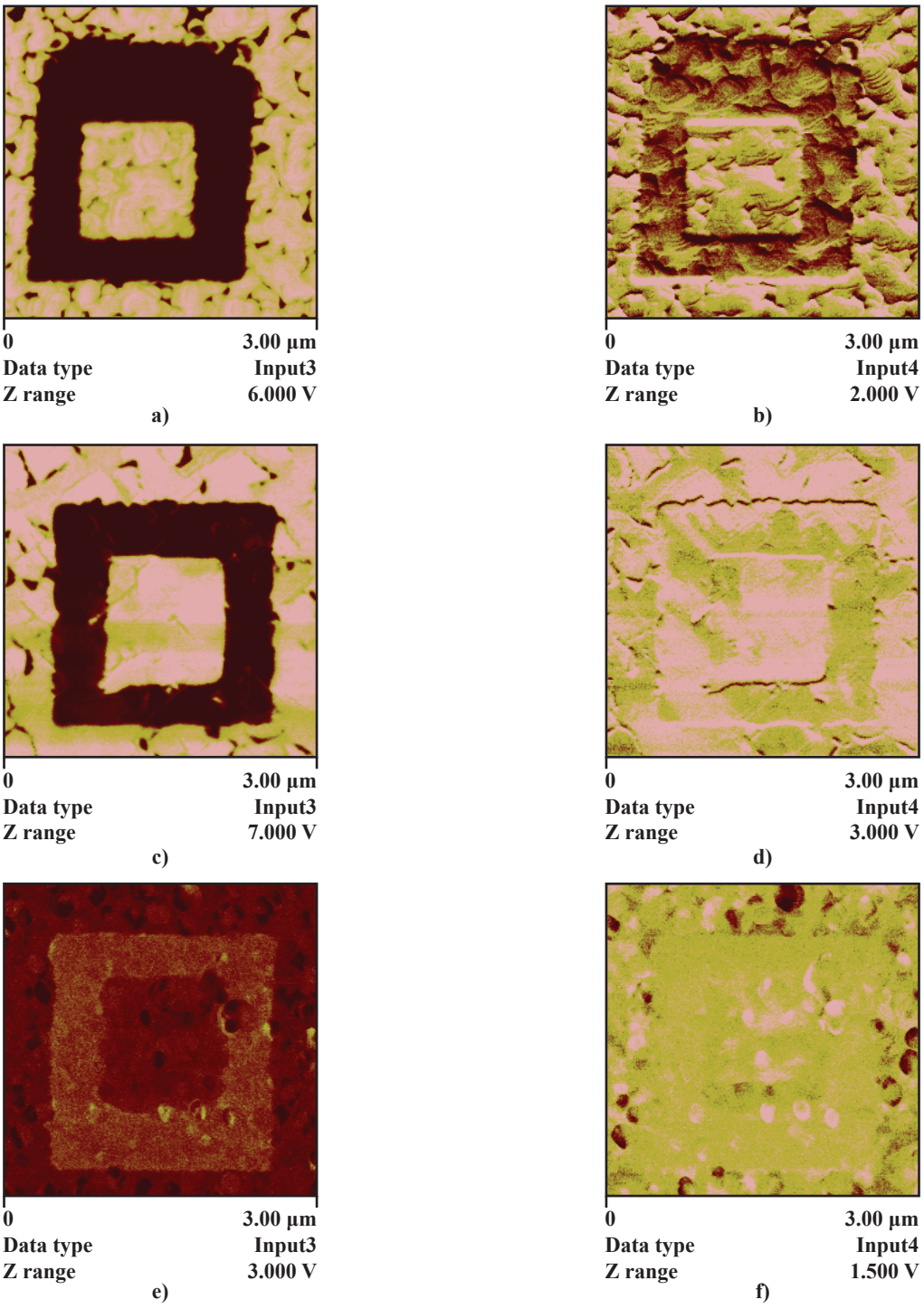

Figure 6. Out-of-plane (OP) and in-plane (IP) PFM images of BZT10:2V ceramics sintered at 1200°C for 2 hours in a conventional furnace. (a) (OP) (N_2) and (b) (IP) (N_2), (c) (OP) (O_2) and (d) (IP) (O_2), (e) (OP) (At_{amb}) and (f) (IP) (At_{amb})

and are illustrated in Fig. 6. The out-of-plane (OP) and in-plane (IP) piezoresponse images of the as-grown sample after applying a bias of –12V, on an area of 2 μm × 2 μm, and then an opposite bias of +12V in the central 1 μm × 1 μm area were employed. To obtain the domain images, a high voltage exceeding the coercive field was applied during scanning. The contrast in these images is associated with the direction of the polarization [32]. The white regions in the out-of-plane PFM images correspond to domains with the polarization vector oriented toward the bottom electrode hereafter referred to as down polarization (Fig. 6a,c,e) while the dark regions correspond to domains oriented upward referred to as up polarization. Grains which exhibit no contrast change are associated with zero out-of-plane polarization. A similar behaviour was observed when a positive bias was applied to the ceramic. We noticed that some of the grains exhibit a white contrast associated to a component of the polarization pointing toward the bottom of the sample. On the other hand, in the in-plane PFM images (Fig. 6b,d,f) the contrast changes were associated with changes of the in-plane polarization components. In this case, the white contrast indicates polarization e.g. in the positive direction of the *y*-axis while dark contrast are given by in-plane polarization components pointing to the negative part of the *y*-axis. The ferroelectric domains consist of a multiple domain state in a mixture of 90° and 180° domains which grow into large blocks. The domains grow in multiple states due to the crystal structure of the BZT10:2V phase. PFM measurements reveal a clear piezoelectric contrast which corresponds to antiparallel domains on all locations tested. There is no reduction in the amplitude of the measured vibrations which is indicative that this phase is still polar and electric field-induced polarization switching still exists. Therefore, our data confirm that the spontaneous polarization is very high in the BZT10:2V sample. Thus, vanadium can reduce the strain energy and pin charged defects. Also, we noted that some of the crystallites apparently have not been switched and still exhibit a positive piezoresponse signal. This result (which can be explained by strong domain pinning in these crystallites) is direct experimental proof that repeated switching results in information about unswitchable polarization which in turn leads to the degradation of switching characteristics.

IV. Conclusions

In summary, we have shown that the nature of BZT10:2V based ceramics defects depends on the annealing atmosphere. XPS data reveal that BZT10:2V ceramic sintered in At_{amb} restrict the movement of Ti^{4+} and Zr^{4+} ions and thus reduce the space charge compensation which leads to a low piezoresponse. The saturation polarization (P_s) and coercive electric field (E_c) of BZT10:2V ceramics were improved under annealing in a nitrogen atmosphere. Meanwhile, BZT10:2V ceramics sintered in oxygen and nitrogen atmospheres exhibited excellent piezoelectric properties which indicate that the oxygen ions environment is quite different among samples. PFM measurements reveal ferroelectric domains growing into large blocks in a mixture of 90° and 180° states. In addition, it is possible that controlling the crystals defects would result in improved piezoeletric properties. The polarization behavior shows that BZT10:2V ceramics are promising for dielectric and ferroelectric applications.

Acknowledgements: The authors are grateful for the financial support of the Brazilian research financing institutions: CAPES, FAPESP and CNPq.

References

1. D. Hennings, A. Schnell, "Diffuse ferroelectric phase-transitions in $Ba(Ti_{1-y}Zr_y)O_3$ ceramics", *J. Am. Ceram. Soc*., **65** (1982) 539–544.
2. V.Ya. Shur, E.B. Blankova, A.L. Subbotin, E.A. Borisova, D.V. Pelegov, S. Hoffmann, D. Bolten, R. Gerhardt, R. Waser, "Influence of crystallization kinetics on texture of sol-gel PZT and BST thin films", *J. Eur. Ceram. Soc.*, **19** (1999) 1391–1395.
3. T. Tsurumi, Y. Yamamoto, H. Kakemoto, S. Wada, H. Chazono, H. Kishi, "Dielectric properties of $BaTiO_3$-$BaZrO_3$ ceramics under a high electric field", *J. Mater. Res.*, **17** (2002) 755–759.
4. U. Weber, G. Greuel, U. Boettger, S. Weber, D. Hennings, R. Waser, "Dielectric properties of $Ba(Zr,Ti)O_3$-based ferroelectrics for capacitor applications", *J. Am. Ceram. Soc.*, **84** (2001) 759–766.
5. D. Hennings, B. Schreinemacher, H. Schreinemacher, "High-permittivity dielectric ceramics with high endurance", *J. Eur. Ceram. Soc*., **13** (1994) 81–88.
6. I.W. Chen, "Structural origin of relaxor ferroelectrics-revisited", *J. Phys. Chem. Solids*, **61** (2000) 197–208.
7. A. Dixit, S.B. Majumder, R.S. Katiyar, "Relaxor behavior in sol–gel-derived $BaZr_{0.40}Ti_{0.60}O_3$ thin films", *Appl. Phys. Lett.*, **82** (2003) 2679–2681.
8. J.A. Sanjurjo, R.S. Katiyar, S.P.S. Porto, "Temperature dependence of dipolar modes in ferroelectric $BaTiO_3$ by infrared studies", *Phys. Review B*, **22** (1980) 2396–2403.
9. Y. Noguchia, M. Miyayama, "Large remanent polarization of vanadium-doped $Bi_4Ti_3O_{12}$", *Appl. Phys. Lett.*, **78** (2001) 1903–1905.
10. F. Moura, A.Z. Simões, L.S. Cavalcante, M. Zampieri, M.A. Zaghete, J.A. Varela, E. Longo, "Strain behaviour of BZT:2%V and BZT:2%W ceramics", *Appl. Phys. Lett.*, **92** (2008) 032905–032907.
11. R. Shannigrahi, R.N.P. Choudhary, N. Acharya, "Electrohydrodynamic instability in 8CB (4'-**n**-octyl-4-cyanobiphenyl) liquid crystal", *Mater. Sci. Eng. B*, **56** (1999) 31–35.

12. D. Bolten, U. Bouger, T. Schneller, M. Grossnam, O. Lose, R. Waser, "Reversible and irreversible processes in donor-doped Pb(Zr,Ti)O_3", *Appl. Phys. Lett.*, **77** (2000) 3830–3832.
13. F. Moura, A.Z. Simões, E.C. Aguiar, I.C. Nogueira, M.A. Zaghete, J.A. Varela, E. Longo. "Dielectric investigations of vanadium modified barium titanate zirconate ceramics obtained from mixed oxide merthod", *J. Alloy. Compd.*, **479** (2009) 280–283.
14. F. Moura, A.Z. Simões, L.S. Cavalcante, M.A. Zaghete, J.A. Varela, E. Longo, "Dielectric and ferroelectric characteristics of barium zirconate titanate ceramics prepared from mixed oxide method", *J. Alloy. Compd.*, **462** (2008) 129–132.
15. B.H. Park, S.J. Hyun, S.D. Bu, T.W. Noh, J. Lee, H.D. Kim, "Difference in nature of defects between $SrBi_2Ta_2O_9$ and $Bi_4Ti_3O_{12}$", *Appl. Phys. Lett.*, **74** (1999) 1907–1909.
16. A.Z. Simões, M.A. Ramirez, A. Ries, R. Ramesh, J.A. Varela, E. Longo, "Electromechanical properties of calcium bismuth titanate films: A potential candidate for lead-free thin-film piezoelectrics", *Appl. Phys. Lett.*, **88** (2006) 072916–072918.
17. M.E. Lines, A.M. Glasss, *Principles and Applications of Ferroelectrics and Related Materials*, Oxford University Press, Oxford 1977.
18. Y. Wu, S. J. Limmer, T. P. Chou, C. Nguyen, C. Guozhong, "Influence of tungsten doping on dielectric properties of strontium bismuth niobate ferroelectric ceramics", *J. Mater. Sci. Lett.*, **21** (2002) 947–949.
19. A.Z. Simões, C.S. Riccardi, A.H.M. Gonzalez, A. Ries, E. Longo, J.A. Varela, "Piezoelectric properties of $Bi_4Ti_3O_{12}$ thin films annealed in different atmospheres", *Mater. Res. Bull.*, **42** (2007) 967–974.
20. A.Z. Simões, M.P. Cruz, A. Ries, E. Longo, J.A. Varela, R. Ramesh, "Ferroelectric and piezoelectric properties of bismuth titanate thin films grown on different bottom electrodes by soft chemical solution and microwave annealing", *Mater. Res. Bull.*, **42** (2007) 975–981.
21. A.Z. Simões, E.C. Aguiar, A. Ries, E. Longo, J.A. Varela, "Niobium doped $Bi_4Ti_3O_{12}$ ceramics obtained by the polymeric precursor method", *Mater. Lett.*, **61** (2007) 588–591.
22. L.S. Cavalcante, A.Z. Simões, L.P.S. Santos, M.R.M.C. Santos, E. Longo, J.A. Varela, "Dielectric properties of $Ca(Zr_{0.05}Ti_{0.95})O_3$ thin films prepared by chemical solution deposition", *J. Solid State Chem.*, **179** (2006) 3739–3743.
23. A.Z. Simões, M.A. Ramírez, B.D. Stojanovic, E. Longo and J.A. Varela, "The effect of microwave annealing on the electrical characteristics of lanthanum doped bismuth titanate films obtained by the polymeric precursor method", *Appl. Surf. Sci.*, **252** (2006) 8471–8474.
24. A.Z. Simões, S. Cava, L.S. Cavalcante, M. Cilense, E. Longo, J.A. Varela, "Ferroelectric and dielectric properties of $Ba_{0.5}Sr_{0.5}(Ti_{0.80}Sn_{0.20})O_3$ thin films grown by the soft chemical method", *J. Solid State Chem.*, **179** (2006) 2972–2976.
25. A.Z. Simões, M.A. Ramírez, E. Longo, J.A. Varela, "Leakage current behavior of $Bi_{3.25}La_{0.75}Ti_3O_{12}$ ferroelectric thin films deposited on different bottom electrodes", *Mater. Chem. Physics.*, **107** (2008) 72–76.
26. L.S. Cavalcante, A.Z. Simões, M.O. Orlandi, M.R.M.C. Santos, J.A. Varela, E. Longo, "Dependence of annealing time on structural and morphological properties of $Ca(Zr_{0.05}Ti_{0.95})O_3$ thin films", *J. Alloy. Compd.*, **453** (2008) 386–391.
27. D.P. Volanti, D. Keyson, L.S. Cavalcante, A.Z. Simões, M.R. Joya, E. Longo, J.A. Varela, P.S. Pizani, A.G. Souza, "Synthesis and characterization of CuO flower-nanostructure processing by a domestic hydrothermal microwave", *J. Alloy. Compd.*, **459** (2008) 537–542.
28. A.Z. Simões, M.A. Ramirez, C.S. Riccardi, E. Longo, J.A. Varela, "Effect of the microwave oven on structural, morphological and electrical properties of $SrBi_4Ti_4O_{15}$ thin films grown on $Pt/Ti/SiO_2/Si$ substrates by a soft chemical method", *Mater. Character.*, **59** (2008) 675–680.
29. D. Keyson, D.P. Volanti, L.S. Cavalcante, A.Z. Simões, J.A. Varela, E. Longo, "CuO urchin-nanostructures synthesized from a domestic hydrothermal microwave method", *Mater. Res. Bull*., **43** (2008) 771–775.
30. L. Wu, C. Wei, T. Wu, H. Liu, "Dielectric properties of modified PZT ceramics", *J. Phys. C: Solid State Phys.*, **16** (1983) 2803–2812.
31. J. Wang, J. B. Neaton, H. Zheng, V. Nagarajan, S. B. Ogale, B. Liu, D. Viehland, V. Vaithyanathan, D.G. Schlom, U.V. Waghmare, M. Wuttig, R. Ramesh, "Epitaxial $BiFeO_3$ multiferroic thin film heterostructures", *Science*, **299** (2003) 1719–1722.
32. A.Z. Simões, A.H.M. Gonzalez, L.S. Cavalcante, C.S. Riccardi, E. Longo, J.A. Varela, "Soft chemical deposition of $BiFeO_3$ multiferroic thin films", *Appl. Phys. Lett.*, **90** (2007) 052906–052908.